IEEE Access
Multidisciplinary | Rapid Review | Open Access Journal

Received December 18, 2018, accepted December 27, 2018, date of publication January 10, 2019, date of current version February 4, 2019.

Digital Object Identifier 10.1109/ACCESS.2019.2891942

An Indoor Position-Estimation Algorithm Using Smartphone IMU Sensor Data

ALWIN POULOSE[1], ODONGO STEVEN EYOBU[1,2], AND DONG SEOG HAN[1]
[1]School of Electronics Engineering, Kyungpook National University, Daegu 41566, South Korea
[2]School of Computing and Informatics Technology, Makerere University, Kampala 7062, Uganda

Corresponding author: Dong Seog Han (dshan@knu.ac.kr)

This work was supported by the Institute for Information and Communication Technology Planning and Evaluation (IITP) funded by the Korean Government (MSIT, Development of Intelligent Interaction Technology Based on Context Awareness and Human Intention Understanding) under Grant R7124-16-0004.

ABSTRACT Position-estimation systems for indoor localization play an important role in everyday life. The global positioning system (GPS) is a popular positioning system, which is mainly efficient for outdoor environments. In indoor scenarios, GPS signal reception is weak. Therefore, achieving good position estimation accuracy is a challenge. To overcome this challenge, it is necessary to utilize other position-estimation systems for indoor localization. However, other existing indoor localization systems, especially based on inertial measurement unit (IMU) sensor data, still face challenges such as accumulated errors from sensors and external magnetic field effects. This paper proposes a position-estimation algorithm that uses the combined features of the accelerometer, magnetometer, and gyroscope data from an IMU sensor for position estimation. In this paper, we first estimate the pitch and roll values based on a fusion of accelerometer and gyroscope sensor values. The estimated pitch values are used for step detection. The step lengths are estimated by using the pitching amplitude. The heading of the pedestrian is estimated by the fusion of magnetometer and gyroscope sensor values. Finally, the position is estimated based on the step length and heading information. The proposed pitch-based step detection algorithm achieves 2.5% error as compared with acceleration-based step detection approaches. The heading estimation proposed in this paper achieves a mean heading error of 4.72° as compared with the azimuth- and magnetometer-based approaches. The experimental results show that the proposed position-estimation algorithm achieves a high position accuracy that significantly outperforms that of conventional estimation methods used for validation in this paper.

INDEX TERMS Indoor positioning system (IPS), pedestrian dead reckoning (PDR), heading estimation, indoor navigation, Android-based smartphone, quaternion, Kalman filter, sensor fusion.

I. INTRODUCTION

Various position estimation techniques exist that can be used to detect the position of pedestrians or objects in indoor or outdoor environments. Such techniques involve the use of global positioning system (GPS) data [1], [2], image data, video data, IMU sensor data, or Wi-Fi data. Although these data can be used in both indoor and outdoor environments, there are highly considerable challenges when data such as GPS, and image or video data are used for indoor localization. These challenges include weak received GPS signals [3], [4], and unpredictable illumination challenges for image or video data [5]. GPS, video, and image data are generally fine for outdoor localization. Therefore, it is necessary to develop new positioning approaches that can offer a higher position accuracy precision. Currently, different indoor positioning systems have been developed. These include wireless local area network (WLAN) [6], ultra-wideband (UWB) communication [7], [8], Wi-Fi-based systems [9]–[11], camera based systems [12], [13], ultrasonic sensors [14], [15], laser-based systems [16], radio frequency identification (RFID) [17]–[20], inertial navigation and inertial measurement unit (IMU)-based navigation systems [21], [22], global system for mobile communications (GSM) [23]–[26], and smartphone-based position-detection systems [27]–[30]. Among these techniques, the smartphone sensor based position-detection system is the most popular. The advantage of using a smartphone-based position-estimation systems is that it requires no additional peripherals devices expect for the smartphone itself. The major applications for smartphone-based Pedestrian dead

reckoning (PDR) systems are localization in shopping malls, airports, tracking firefighters or soldiers, underground parking areas, and personal locators in tunnels and GPS-denied outdoor environments. Another advantage of the smartphone-based position-estimation system is that it uses only one system instead of integrating WiFi signals, radio frequency signals, GPS, or vision cameras. The integration of other system increases the system cost and complexity. Integration of WiFi signals and vision cameras require installation and maintenance of the infrastructure. Based on only a smartphone, this paper proposes a sensor fusion technique for pitch and roll estimation, a pitch-based step detection algorithm, a sensor fusion for heading estimation (HD) and a position estimation algorithm. Experiments were conducted in three different indoor scenarios and showed a better positioning accuracy compared to other conventional approaches. The main contributions of this paper are as follows:

- We designed a Kalman filter algorithm for sensor fusion. The proposed system uses two sensor fusion algorithms for position estimation. We implemented first sensor fusion algorithm for pitch and roll estimation and second sensor fusion algorithm for heading estimation. The proposed system uses the accelerometer and gyroscope data for pitch and roll estimation and magnetometer and gyroscope data for heading estimation.
- We proposed a pitch-based step detection algorithm for detecting steps. We analyzed the proposed step detection approach with acceleration based step detection approaches.
- We formulated a position estimation algorithm and compared the results with conventional PDR approach.

This paper is organized as follows. In Section II, a review of previous work is presented. Section III discusses the smartphone coordinate system. The proposed position-estimation algorithm is discussed in Section IV. The analysis of both the experiments and results is provided in Section V. Finally, the conclusions and future work are summarized in Section VI.

II. RELATED WORK

Position estimation has been studied in the past and recently for applications in object detection, robotics, and various tracking purposes. The discussion of this section focuses on related work for position estimation. The position-estimation study is related to two research areas: step detection and heading estimation. The final area of study related to position estimation is sensor-fusion technologies. Various sensor-fusion techniques are used for position estimation for better performance.

The performance of position estimation algorithms depends on the accuracy of step detection. It is necessary to estimate the steps and the step length (SL) of the pedestrian for accurate position estimation. Conventional step detector algorithms use accelerometer sensor data to detect steps. Ahmad *et al.* [31] studied the fundamental analysis of step-detection algorithms and discussed their performance based on dynamic step lengths. Ho *et al.* [32] reported an adaptive step length estimator. In their proposed method, a fast Fourier transform (FFT)-based smoother on the acceleration data instead of conventional filtering methods such as high pass and low pass filters was used. Experimental results showed that the proposed method achieves better performance compared to the conventional estimation methods. Another approach for step detection and step length estimation is to use a neural network. Liu *et al.* [33] explained the neural network concept for step detection. In their paper, they describe a compositional algorithm of empirical formula and back-propagation neural network to estimate step length. In this paper, we propose a pitch based step detection algorithm instead of accelerometer-based step detections. The proposed pitch-based approach uses the pitch angle for step detection and estimates the step length based on the pitch amplitude.

The performance of the position estimation also depends on the accurate heading estimation. Magnetometer and gyroscope sensors are used for estimating heading. Yuan *et al.* [34] introduced a quaternion-based, unscented Kalman filter for accurate indoor heading estimation. In their work, a wearable multisensory system with different sensors was utilized. The experimental results show that the designed system has high heading accuracy with respect to the ground truth-values. Renaudin *et al.* [35] explain about a quaternion-based heading estimation method and proposed magnetic angular rate update and acceleration gradient update. The experimental results show that the proposed method reduces the heading error compared to other methods. The accuracy of the heading depends on the position in which the smartphone is held. Liu *et al.* [36] discusses smartphone-holding postures for heading estimation and have proposed a heading estimation algorithm for different smartphone holding postures. In this study, we use magnetometer and gyroscope sensors. The magnetometer is easily affected by an external disturbance and the gyroscope values are not reliable for long-duration experiments. To overcome these issues, we use the sensor-fusion technique in our algorithm. Quaternion updated gyroscope values are used for reducing the drift problems.

The position is estimated from combining step length and heading information. In Ali and El-Sheimy [37], a basic position-estimation algorithm is explained. Ali and El-Sheimy [37] introduced a sensor-fusion technique for position estimation. The proposed position algorithm has less than 15 m position error in a harsh environment. In this study, we have considered the same experiment scenario and our algorithm achieves less than 2.6 m of position error as compared to results achieved in [37]. In Kang and Han [38], a smartphone-based PDR for an indoor localization was presented. Experimental results show that their proposed system has reasonable location accuracy. Tian *et al.* [39] deals with a multi-mode dead reckoning system for pedestrian tracking using smartphones. Their work introduces a mode detection for the PDR system. The mode represents a specific state of carrying a mobile device, and it is

automatically detected during pedestrian walk. The mode detection algorithm improves position-detection performance. Their proposed system achieves real-time tracking and localization performance with high positional accuracy. Another way to improve on the performance of a pedestrian navigation system is to create a motion recognition algorithm. Shin *et al.* [40] explain the use of motion recognition-based 3D pedestrian navigation system using a smartphone. This paper proposes an android-based PDR system. The experimental results show that the proposed method has a high positioning accuracy as compared to the conventional PDR systems.

The position-estimation systems discussed here require further improvement related to position accuracy. Therefore, it is necessary to propose a new position-estimation algorithm for different indoor conditions. This paper proposes a position-estimation algorithm for different indoor scenarios. The proposed algorithm is validated by three experiment scenarios. The accuracy of the proposed algorithm is assessed and evaluated by computing the displacement error and root mean square error (RMSE). The experiment result shows that the proposed algorithm has higher positional accuracy as compared to conventional method.

III. SMARTPHONE COORDINATE SYSTEM

In usual, smartphone sensors use a standard 3-axis coordinate system to express data values. The smartphone coordinate system is defined relative to the device's screen when the device is held in its default orientation. Fig. 1 shows the coordinate system used in the smartphone [41].

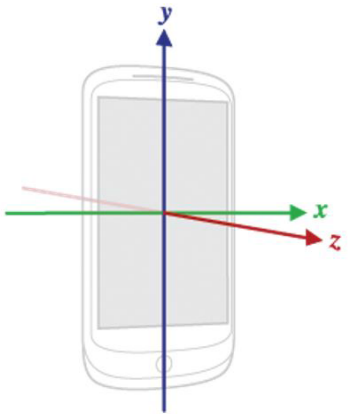

FIGURE 1. Smartphone coordinate system (relative to a device).

When the device is in its normal position, the x axis is horizontal and points to the right, the y axis is vertical and points up, and the z axis points out from the face of the screen. In this coordinate system, locations behind the screen are represented by negative z values. Smartphone sensors, like the accelerometer, magnetometer, and gyroscope, use these coordinate systems. The important point of this coordinate system is that the axes are not swapped when the device's screen orientation changes. This means that the sensor's coordinate system never changes as the device moves. The rotation matrix R from the android operating system is defined by

$$\boldsymbol{R} = \begin{bmatrix} E_x & E_y & E_z \\ N_x & N_y & N_z \\ G_x & G_y & G_z \end{bmatrix} \tag{1}$$

where x, y and z are axes relative to the smartphone and $\boldsymbol{E}, \boldsymbol{N}, \boldsymbol{G}$ defined as follows:

$\boldsymbol{E} = (E_x, E_y, E_z) =$ a unit vector that points East.

$\boldsymbol{N} = (N_x, N_y, N_z) =$ a unit vector that points North.

$\boldsymbol{G} = (G_x, G_y, G_z) =$ a unit vector that points away from the center of the earth (gravity vector).

The Euler angles Φ, θ and ψ are expressed as

$$\text{azimuth} = \psi = \text{rotation about } \boldsymbol{G}.$$
$$\text{pitch} = \theta = \text{rotation about } \boldsymbol{E}.$$
$$\text{roll} = \Phi = \text{rotation about } \boldsymbol{N}.$$

When the smartphone is not in the normal position, it is necessary to remove the tilting effect. To remove the titling effect, the proposed algorithm transforms the original acceleration data from smartphone coordinates to earth coordinate system. The rotation matrices of the azimuth ($\boldsymbol{R}_\psi$), pitch ($\boldsymbol{R}_\theta$), and roll ($\boldsymbol{R}_\phi$) are expressed as [51]

$$\boldsymbol{R}_\psi = \begin{bmatrix} \cos\psi & \sin\psi & 0 \\ -\sin\psi & \cos\psi & 0 \\ 0 & 0 & 1 \end{bmatrix} \tag{2}$$

$$\boldsymbol{R}_\theta = \begin{bmatrix} 1 & 0 & 0 \\ 0 & \cos\theta & \sin\theta \\ 0 & -\sin\theta & \cos\theta \end{bmatrix} \tag{3}$$

$$\boldsymbol{R}_\phi = \begin{bmatrix} \cos\phi & 0 & \sin\phi \\ 0 & 1 & 0 \\ -\sin\phi & 0 & \cos\phi \end{bmatrix} \tag{4}$$

The relationship between the rotation matrix and Euler angles is given by (5) and (6) [51]. The transformation of the acceleration data from smartphone coordinate (a_x, a_y, a_z) to earth coordinate (A_x, A_y, A_z) is given by

$$\begin{bmatrix} A_x \\ A_y \\ A_z \end{bmatrix} = \boldsymbol{R}_{(\psi,\theta,\phi)} \begin{bmatrix} a_x & a_y & a_z \end{bmatrix}^T \tag{7}$$

The acceleration in the earth coordinates is free from tilting effect, however, the z-axis component of the acceleration contains gravity, and the proposed algorithm removes the effect of gravity with (8).

$$\boldsymbol{A}_{\text{linear}} = \begin{bmatrix} A_x \\ A_y \\ A_z \end{bmatrix} - g \begin{bmatrix} 0 & 0 & 1 \end{bmatrix}^T \tag{8}$$

where $\boldsymbol{A}_{\text{linear}}$ is the linear acceleration and the parameter $g = 9.80\ m/s^2$ is the gravitational acceleration.

IV. PROPOSED POSITION-ESTIMATION ALGORITHM FOR INDOOR LOCALIZATION

Positions in indoor scenarios can be estimated in different ways. The conventional position-estimation algorithms use the gyroscope integration process for heading estimation [43]. This process creates an accumulated error from gyroscope and this affects positioning accuracy. Another conventional approach is to estimate the heading based on the magnetometer. Magnetometer-based heading estimation is not reliable for experiments that span over a long time. Fig. 2 shows the conventional position-estimation method using both the accelerometer and gyroscope sensor information.

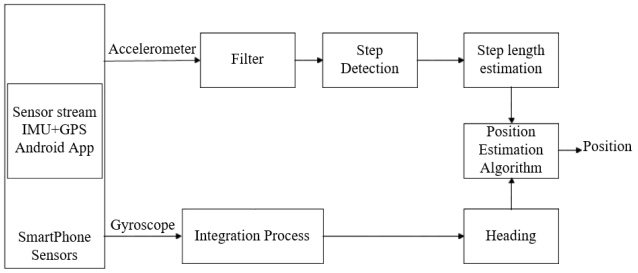

FIGURE 2. Conventional position estimation method using accelerometer and gyroscope sensors.

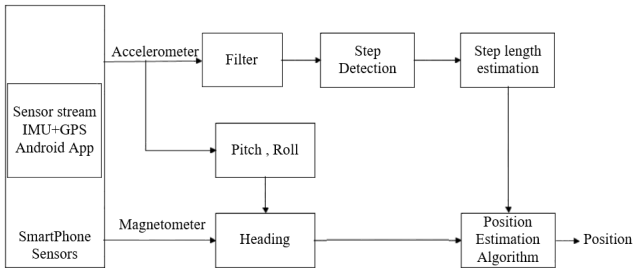

FIGURE 3. Conventional position estimation method using accelerometer and magnetometer sensors.

In order, to overcome the accumulated error when using only the gyroscope, the magnetometer data is introduced to the system [44]. Fig. 3 shows the conventional position-estimation method using accelerometer and magnetometer sensors. However, the magnetometer is also not reliable since magnetometers are easily affected by external magnetic fields hence affecting positioning accuracy.

The proposed position-estimation algorithm uses a combination of the accelerometer, magnetometer, and gyroscope sensor readings. Fig. 4 shows the proposed position-estimation algorithm. For the comparison of our results, we compared the proposed system results with the position-estimation results when both the accelerometer and magnetometer sensors are used.

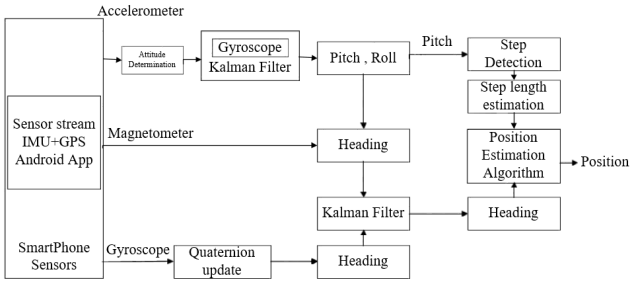

FIGURE 4. Smartphone-based position estimation.

The experiments were conducted using smartphone sensors with acceleration, gyroscope, and magnetometer data. For data collection, the sensor stream inertial measurement unit and global positioning system android application is used. The android application deals with hard-and software sensors integrated in smartphones. The pedestrian can select the sensors and observe the current values of accelerometer, gyroscope, and magnetometer. A stream containing the sensor values in comma-separated values (CSV) format can be stored on an secure digital (SD) card or internal storage of a smartphone. The application provides an option for sensor-update frequency adjustments.

The proposed position-estimation algorithm is divided into different stages. The first stage of the proposed algorithm is to calculate the pitch and roll. The estimated pitch values are used for step detection. The second stage of the proposed algorithm is to estimate the step length. The model presented in [45] is used for step length estimation. The third stage of the proposed algorithm is to estimate the heading. The heading estimation algorithm uses the magnetometer and gyroscope data to estimate the heading. The final stage of the proposed algorithm is to estimate the position. The position is estimated from the step length and heading information.

A. PITCH AND ROLL ESTIMATION BASED ON SENSOR FUSION

Sensor-fusion is used for calculating the pitch and roll values. Sensor fusion is a technique used to combine different sensors. The proposed algorithm combines the accelerometer and gyroscope data for roll and pitch estimation.

$$\boldsymbol{R}_{(\psi,\theta,\phi)} = \begin{bmatrix} \cos\psi & \sin\psi & 0 \\ -\sin\psi & \cos\psi & 0 \\ 0 & 0 & 1 \end{bmatrix} \begin{bmatrix} 1 & 0 & 0 \\ 0 & \cos\theta & \sin\theta \\ 0 & -\sin\theta & \cos\theta \end{bmatrix} \begin{bmatrix} \cos\phi & 0 & \sin\phi \\ 0 & 1 & 0 \\ -\sin\phi & 0 & \cos\phi \end{bmatrix} \tag{5}$$

$$\boldsymbol{R}_{(\psi,\theta,\phi)} = \begin{bmatrix} \cos\phi\cos\psi - \sin\phi cos\theta sin\psi & \cos\phi\sin\psi + \sin\phi\cos\theta\cos\psi & \sin\phi\sin\theta \\ -\sin\phi\cos\psi - \cos\phi\cos\theta\sin\psi & -\sin\phi\sin\psi + \cos\phi\cos\theta cos\psi & \cos\phi\sin\theta \\ \sin\theta\sin\psi & -\sin\theta\cos\psi & \cos\theta \end{bmatrix} \tag{6}$$

This technique removes the accumulated error from both the accelerometer and gyroscope. The idea behind this approach is that, since the gyroscope-based position accuracy result is good in a short time span and the accelerometer-based position accuracy result is good for a longer time span, combining both accelerometer and gyroscope features achieves better performance on positioning accuracy in a longer time span.

1) CALCULATION OF PITCH AND ROLL FROM ACCELEROMETER

The three-axis acceleration data in the device coordinate systems are $a_{acc} = (a_x, a_y, a_z)$ and g denotes gravity acceleration. The pitch and roll angles are given by

$$\text{Pitch angle}(\theta) = \sin^{-1}\left(\frac{a_y}{g}\right) \tag{9}$$

$$\text{Roll angle}(\phi) = \tan^{-1}\left(\frac{a_x}{a_z}\right) \tag{10}$$

2) CALCULATION OF PITCH AND ROLL FROM GYROSCOPE

In the calculation of the pitch and roll angles using gyroscope sensor data, the angular velocities measured from gyroscope are integrated with respect to time.

3) SENSOR FUSION

Sensor-fusion helps to reduce on the accumulated error from the accelerometer. The accelerometer exhibits a limited range of error when the sensor-fusion approach is applied. The expression used for calculation of the pitch and roll angles from the accelerometer is an approximation valid only in situations when the acceleration or angular rate is small. When we consider the gyroscope pitch and roll angles, the error is accumulated after numerical integration. Sensor-fusion removes the error from the accelerometer and gyroscope and it results in better performance. A Kalman filter [46] with a suitable system model that combines the complementary features of the gyroscope and accelerometer as seen in Fig. 5 is used for sensor fusion. Gyroscope quaternion values are used as the state variable, which is given by

$$\boldsymbol{x} = [\,q_0 \quad q_1 \quad q_2 \quad q_3\,]^T \tag{11}$$

The three-axis gyroscope data in the device coordinate systems are $(\omega_x, \omega_y, \omega_z)$ and the quaternion-based state update is given by

$$\dot{\boldsymbol{q}} = \frac{1}{2}\begin{bmatrix} 0 & -\omega_x & -\omega_y & -\omega_z \\ \omega_x & 0 & \omega_z & -\omega_y \\ \omega_y & -\omega_z & 0 & \omega_x \\ \omega_z & \omega_y & -\omega_x & 0 \end{bmatrix}\begin{bmatrix} q_0 \\ q_1 \\ q_2 \\ q_3 \end{bmatrix} \tag{12}$$

The system model matrix $\boldsymbol{A}$ is defined as

$$\boldsymbol{A} = \frac{1}{2}\begin{bmatrix} 0 & -\omega_x & -\omega_y & -\omega_z \\ \omega_x & 0 & \omega_z & -\omega_y \\ \omega_y & -\omega_z & 0 & \omega_x \\ \omega_z & \omega_y & -\omega_x & 0 \end{bmatrix} \tag{13}$$

The state variable is defined by the gyroscope quaternion values. Therefore, it is necessary to convert the gyroscope data

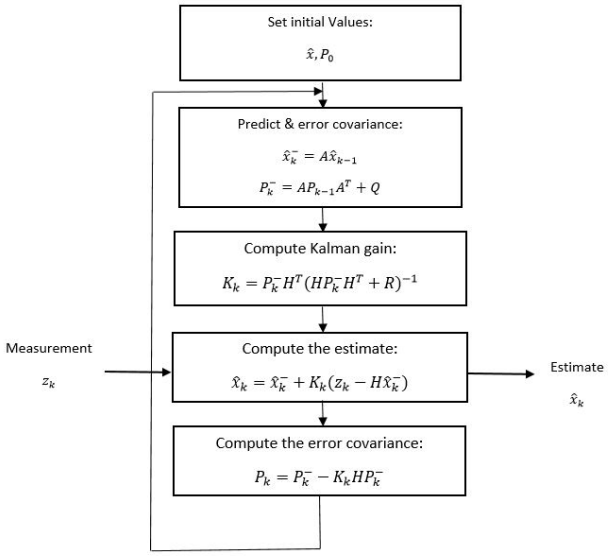

FIGURE 5. Kalman Filter algorithm.

to quaternion values [34]. The conversion of the gyroscope Euler angles to quaternion values are given by

$$\begin{bmatrix} q_0 \\ q_1 \\ q_2 \\ q_3 \end{bmatrix} = \begin{bmatrix} \cos\frac{\phi}{2}\cos\frac{\theta}{2}\cos\frac{\psi}{2} + \sin\frac{\phi}{2}\sin\frac{\theta}{2}\sin\frac{\psi}{2} \\ \sin\frac{\phi}{2}\cos\frac{\theta}{2}\cos\frac{\psi}{2} - \cos\frac{\phi}{2}\sin\frac{\theta}{2}\sin\frac{\psi}{2} \\ \cos\frac{\phi}{2}\sin\frac{\theta}{2}\cos\frac{\psi}{2} + \sin\frac{\phi}{2}\cos\frac{\theta}{2}\sin\frac{\psi}{2} \\ \cos\frac{\phi}{2}\cos\frac{\theta}{2}\sin\frac{\psi}{2} - \sin\frac{\phi}{2}\sin\frac{\theta}{2}\sin\frac{\psi}{2} \end{bmatrix} \tag{14}$$

The accelerometer measurements are used to calculate the quaternion updated values and the result of above equation is used as the measurement (z_k) for the Kalman filter. Through analyzing several experiment results for Kalman filter, this paper assigns the following values for filter variables.

The $\boldsymbol{H}$ matrix is given by

$$\boldsymbol{H} = \begin{bmatrix} 1 & 0 & 0 & 0 \\ 0 & 1 & 0 & 0 \\ 0 & 0 & 1 & 0 \\ 0 & 0 & 0 & 1 \end{bmatrix} \tag{15}$$

The noise covariance matrices $\boldsymbol{Q}$ and $\boldsymbol{R}$ are expressed as

$$\boldsymbol{R} = \begin{bmatrix} 0.0001 & 0 & 0 & 0 \\ 0 & 0.0001 & 0 & 0 \\ 0 & 0 & 0.0001 & 0 \\ 0 & 0 & 0 & 0.0001 \end{bmatrix} \tag{16}$$

$$\boldsymbol{Q} = \begin{bmatrix} 0.001 & 0 & 0 & 0 \\ 0 & 0.001 & 0 & 0 \\ 0 & 0 & 0.001 & 0 \\ 0 & 0 & 0 & 0.001 \end{bmatrix} \tag{17}$$

The initial value for the state variable is given by the following form

$$\widetilde{\boldsymbol{x}} = [\,1 \quad 0 \quad 0 \quad 0\,]^T \tag{18}$$

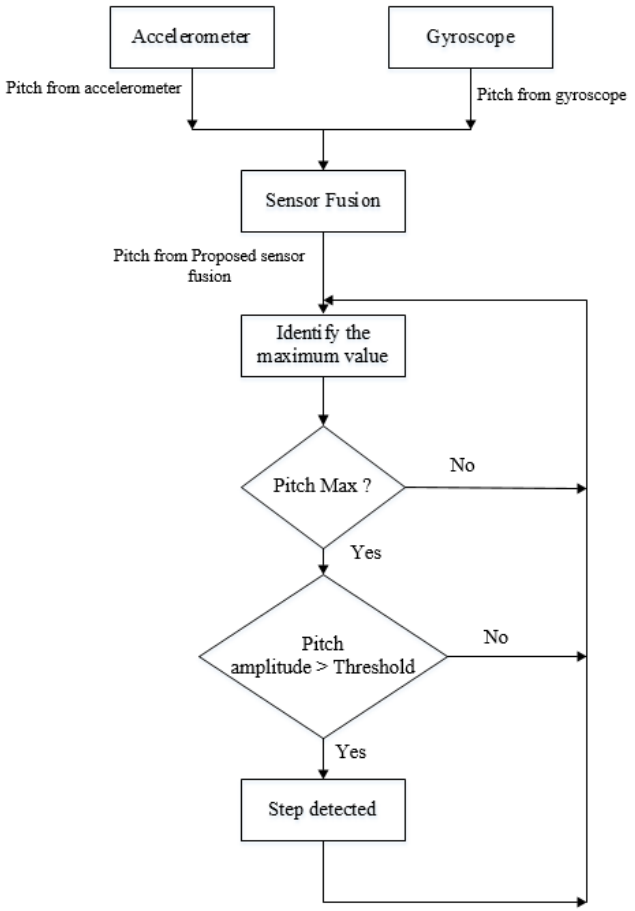

FIGURE 6. Proposed pitch-based step detector.

The error covariance matrix is represented by following form

$$\boldsymbol{P}_0 = \begin{bmatrix} 1 & 0 & 0 & 0 \\ 0 & 1 & 0 & 0 \\ 0 & 0 & 1 & 0 \\ 0 & 0 & 0 & 1 \end{bmatrix} \tag{19}$$

B. STEP DETECTION

The estimated pitch values from sensor fusion technique are used for step detection. The idea of pitch-based step detection was explained in [45]. The proposed step detection algorithm analyses the pitch and detects the step when a maximum pitch value occurs. The block diagram of proposed pitch-based step detector is shown in Fig. 6. The pitch used as the sensor fusion inputs are from both the accelerometer and gyroscope. The maximum and minimum values of fused pitch is identified, a step is detected when a valid maximum peak (Maxima) and a valid minimum peak (Minima) are detected in a sequence in a certain interval. To avoid false step detection, a step is only detected if the pitch value is above a defined threshold value. The maxima is a maximum peak that exceeds upper threshold, while minima is the minimum peak lower than the lower threshold. The upper threshold is determined by summing last valid minima with a Δ threshold value, while the lower threshold is determined by subtracting last valid maxima with a Δ threshold value, an interval time difference between maxima and minima is also determined experimentally, must be between 110ms - 400ms in order to ensure a valid step [54].

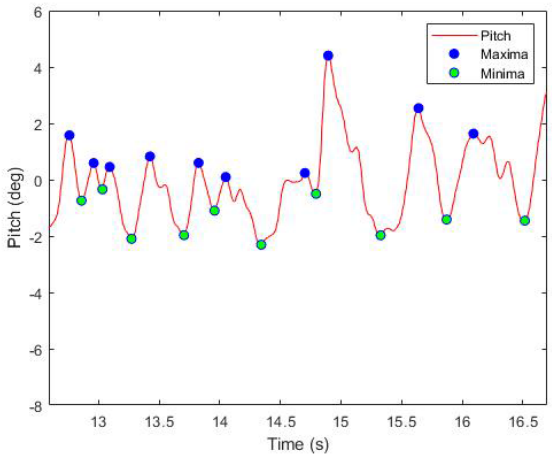

FIGURE 7. Example of step detection.

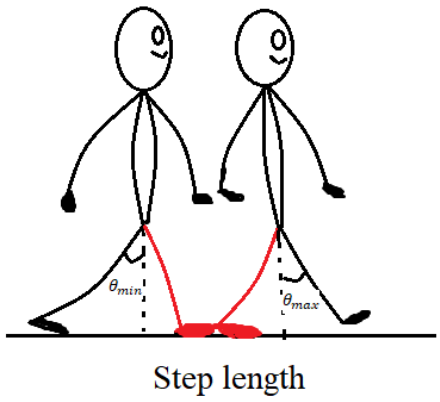

FIGURE 8. The legs during the occurrence of a step.

In Fig. 7 the pitch obtained from a pedestrian walking with the smartphone in his hand is shown. In the figure, a total of 10 steps are represented. This demonstrates the cyclic nature of the steps during the walk is easily identifiable. The highest positive peak $\theta_{\max}$, corresponds to the maximum leg's elongation when walking and the second positive peak occurs as a consequence of the foot hitting the floor. $\theta_{\min}$ is the lowest and unique negative peak. A step is illustrated by the two leg-motion in Fig. 8. The black leg indicates the smartphone is in the left hand of the pedestrian and a step is considered between hits on the floor of this leg. The vertical dashed line represents a pitch equal to zero. When the pitch angle crosses first to zero in Fig. 7 the black leg overtakes the red leg. When the pedestrian is standing the legs are closed, thus the opening angle is zero. By observing Fig. 7, it is clear that, because of the knee, $\theta_{\max}$ is much greater than $\theta_{\min}$ [45].

C. STEP LENGTH ESTIMATIONN

The step length estimation algorithm follows the model presented in [45] to estimate the step length. The step length model estimates the step length through a first-order linear regression model on the pitch amplitude ($\Delta\theta$) and is given by [45]

$$SL = a \times \Delta\theta + b \tag{20}$$

where $\Delta\theta$ is the difference between highest positive peak ($\theta_{\max}$) and lowest negative peak ($\theta_{\min}$), in degrees. The constants a and b are the personalized parameters fitting each regression line.

D. HEADING ESTIMATION

The other important information used for position-estimation is the heading. Heading estimation is the process of determining the direction of pedestrian movements. Two smartphone sensors are used to determine the heading in our proposed system. Both are used for purposes of error reduction especially during a long time span [47]. The relation between magnetic strength in the device (h_x, h_y, h_z) and global (H_x, H_y, H_z) coordinate system is expressed as

$$\begin{bmatrix} H_x \\ H_y \\ H_z \end{bmatrix} = \begin{bmatrix} \cos\phi & \sin\phi\sin\theta & -\sin\phi\cos\theta \\ 0 & \cos\theta & \sin\theta \\ \sin\phi & -\sin\theta\cos\phi & \cos\phi\cos\theta \end{bmatrix} \begin{bmatrix} h_x \\ h_y \\ h_z \end{bmatrix} \tag{21}$$

Heading γ is then given by

$$\gamma = \tan^{-1}\left(\frac{H_y}{H_x}\right) \tag{22}$$

The gyroscopic heading shows better results than the magnetometer heading. Let ω_x represent the body-frame x-axis gyro output, ω_y represent the body-frame y-axis gyro output, and ω_z represent the body-frame z-axis output. Then, the Euler angles are computed as [34]

$$\begin{bmatrix} \omega_x + \omega_y\sin(\phi)\tan(\theta) + \omega_z\cos(\phi)\tan(\theta) \\ \omega_y\cos(\phi) - \omega_z\sin(\phi) \\ \omega_y\sin(\phi)/\cos(\theta) + \omega_z\cos(\phi)/\cos(\theta) \end{bmatrix} = \begin{bmatrix} \dot{\phi} \\ \dot{\theta} \\ \dot{\psi} \end{bmatrix} \tag{23}$$

The quaternion update values are expressed by (14). The gyroscopic heading is obtained by following equation.

$$\text{Heading}_{\text{gyro}} = \arctan\left[\frac{2(q_0q_3 + q_1q_2)}{1 - 2(q_2^2 + q_3^2)}\right] \tag{24}$$

The proposed position-estimation algorithm uses the results from (22) and (24) for sensor-fusion. The results from the sensor fusion show that it has less heading error than the azimuth-based and magnetometer-based heading-estimation methods.

Assume S_t is the heading direction and γ is the input of the system. The state transition function of the heading fusion framework is expressed as [55]

$$S_t = AS_{t-1} + B\gamma + w \tag{25}$$

where A and B are identity matrices and w denotes the Gaussian noise of the system with zero mean and variance ϕ . The observation of the system comes from the gyroscope sensor output, $O_t = \arctan\left[\frac{2(q_0q_3+q_1q_2)}{1-2(q_2^2+q_3^2)}\right]$. The observation function can be expressed as

$$O_t = CS_t + r \tag{26}$$

where $C = \begin{bmatrix} 1 & 0 \end{bmatrix}$ and r denotes the Gaussian noise of the magnetometer output with zero mean and variance φ.

The Kalman filter [46] is applied to solve this problem and the system contains two parts:

1) PREDICTING

$$S_t = AS_{t-1} + B\gamma \tag{27}$$

$$P_t = AP_{t-1}A^T + \phi \tag{28}$$

2) Updating

$$K_t = P_tC^T(CP_tC^T + \varphi)^{-1} \tag{29}$$

$$S_t = S_{t-1} + K_t(O_t - CS_{t-1}) \tag{30}$$

$$P_t = P_t - KCP_t \tag{31}$$

E. POSITION ESTIMATION

The final stage of the proposed algorithm is to estimate the position using the step length and heading information. The current position of the pedestrian is calculated from the previously known position, step length information and the heading from a step interval [48]. The initial position of the pedestrian is defined and using the step length and heading information calculate the current position of the pedestrian. The proposed algorithm assumes the initial position of the pedestrian as zero. The position is expressed as

$$X_t = X_{t-1} + SL \times \cos(HD) \tag{32}$$

$$Y_t = Y_{t-1} + SL \times \sin(HD) \tag{33}$$

where X_t, Y_t are the position values and X_{t-1}, Y_{t-1} are the initial position values. To determine the absolute position of the pedestrian, QR code, RFID, UWB, and computer vision navigation methods are used.

V. EXPERIMENTS AND RESULT ANALYSIS

To evaluate the performance and accuracy of our proposed position-estimation algorithm, we considered three-experiment scenarios such as rectangular motion, straight-line motion, and circular motion of pedestrian as shown in Fig. 9. The data are collected at the fifth floor of IT building 1, Kyungpook National University, South Korea. During data collection the pedestrian (Age 27, Height 172 cm) held the smartphone in his hand and walked in the reference path. The red lines in the Fig. 9 indicated the reference paths for all experiments.

The experiment is carried out in an Android 7.1.1 Nougat platform on a Samsung Galaxy Note 8 smartphone with Snapdragon 835 processor and 6 GB RAM. Through analysing

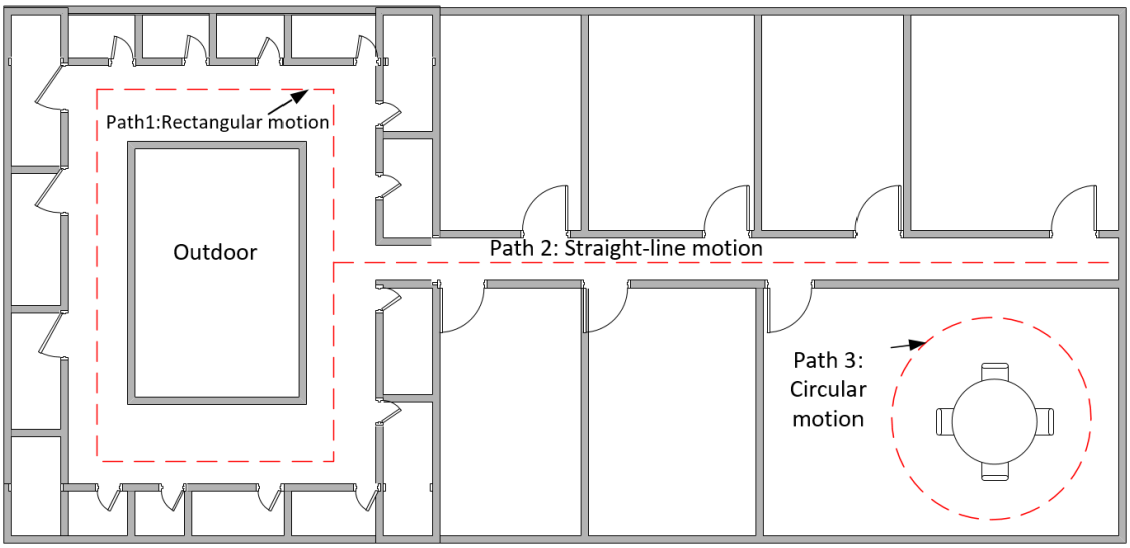

FIGURE 9. Experiment scenarios.

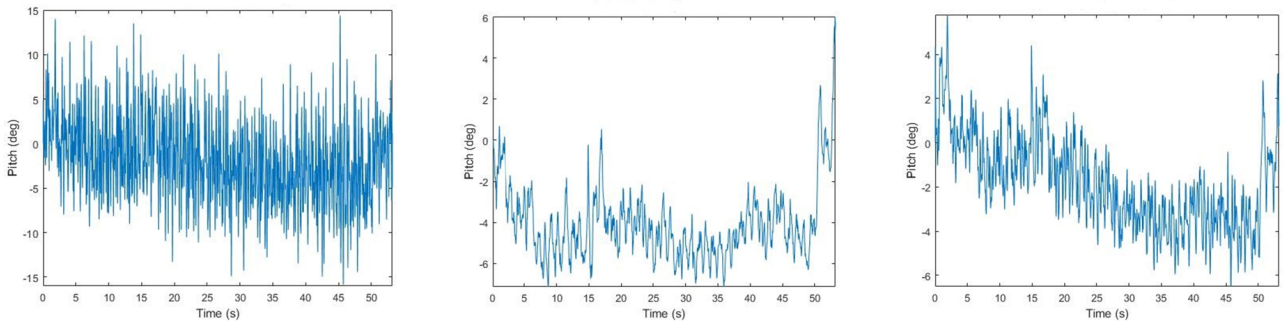

FIGURE 10. Pitch values. (a) Accelerometer. (b) Gyroscope. (c) Proposed method.

several experiment results, this paper assigns the upper and lower threshold for step detection to be 0.5. The performance of proposed position-estimation algorithm is evaluated through extensive experiment scenarios and results. First the pitch and roll estimation, heading estimation, and position-estimation are executed and the performance are evaluated.

To analyse the effect of proposed sensor fusion for pitch and roll estimation, the data in the path 2 is chosen and the Figs. 10 and 11 show the pitch and roll values from the accelerometer, gyroscope and proposed method. From the figures, it can be seen that the proposed sensor fusion approach removed the effect of accumulated error from accelerometer and drift error from gyroscope. The dc offset from the accelerometer is suppressed by proposed sensor fusion method. The proposed sensor fusion results are less fluctuating than independent sensor results and makes the best performance for step detection algorithm. The estimated pitch values from sensor fusion are used for pedestrian step detection.

To evaluate the performance of step detection, the proposed pitch-based step detection is compared with acceleration-based step detection approaches. The data of holding smartphone in hand in path 2 is chosen to compare the proposed pitch-based step detection approach with acceleration-based step detection approaches. The number of steps in path 2 is 127. The relative error to evaluate the performance is defined as [42]

$$e = \frac{|N_e - N_r|}{N_r} \times 100\% \tag{34}$$

where N_e is the number of detected steps, and N_r is the ground truth. The TABLE 1 shows the accuracy comparison of proposed step detection with acceleration based approaches. In TABLE 1, the proposed pitch-based step detection approach is compared with acceleration-based step detection approaches such as peak detection approach, zero crossing detection approach and Samsung health android application approach.

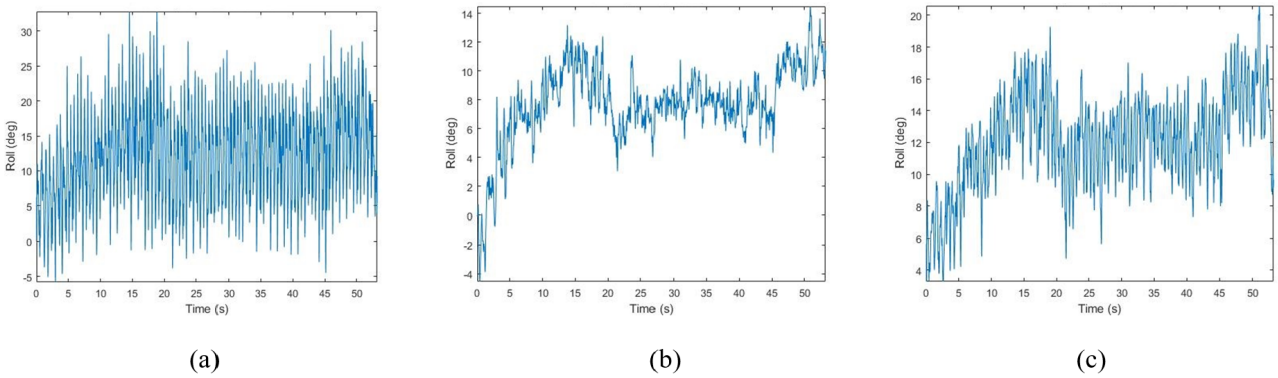

FIGURE 11. Roll values. (a) Accelerometer. (b) Gyroscope. (c) Proposed method.

TABLE 1. Accuracy comparison of different step detection approaches.

Approach	Error
Proposed pitch-based approach	3.14%
Zero crossing detection approach	10.23%
Peak detection approach	18.11%
Samsung health android application approach	21.25%

From TABLE 1, it is clear that the proposed pitch-based approach has better performance than acceleration-based approaches. The zero-crossing approach (ZC) shows a better performance than the peak detection (PD) and the Samsung health android application approach. The error analysis shows that the Samsung health android application has very poor performance than other approaches and it is not suitable for PDR localization.

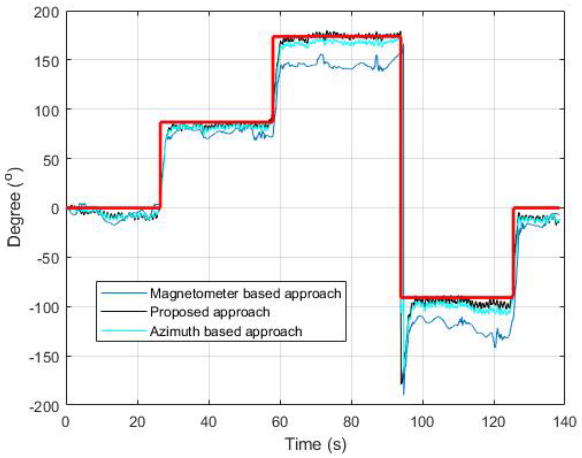

FIGURE 12. Performance comparison of heading estimation.

Path1 rectangular motion of pedestrian is chosen to evaluate the performance of proposed heading estimation algorithm. It consist of four direction paths. The proposed heading estimation algorithm uses the sensor fusion technique for estimating the direction. We compare the proposed heading estimation with azimuth based and magnetometer based approaches. The heading from all approaches are shown in Fig. 12. The red line in the Fig. 12 indicates the ground truth values of heading.

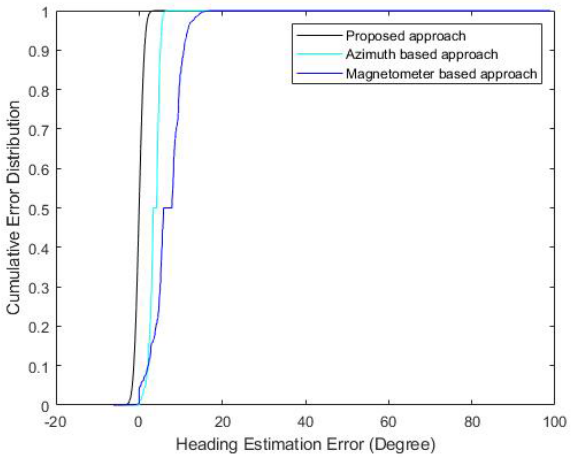

FIGURE 13. Heading estimation error Distribution.

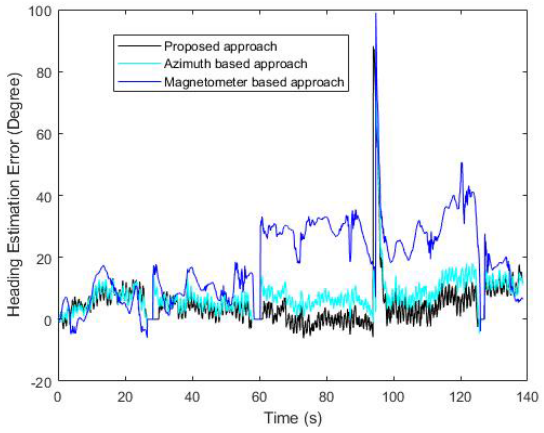

FIGURE 14. Heading error estimation.

From Fig. 12, it can be seen that the proposed heading estimation algorithm can avoid the effect of sensor errors. The performance of proposed heading fusion technique is evaluated by a cumulative error distribution function and heading error. Fig. 13 shows the cumulative heading error distributions of the three approaches. The proposed heading estimation approach achieves the best performance in all the three heading estimation approaches. The azimuth

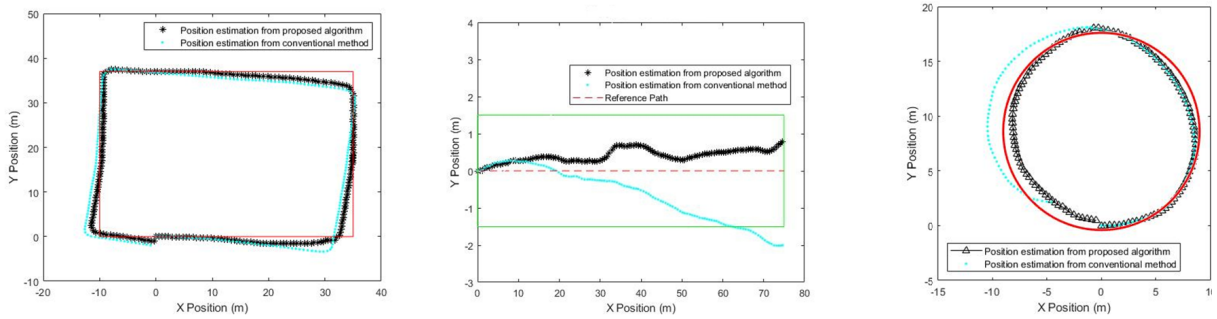

FIGURE 15. Trajectories of the ground truth, the conventional PDR approach and proposed PDR approach in different experiment scenarios. (a) Rectangular motion. (b) Straight-line motion. (c) Circular motion.

heading approach is better than the magnetometer based approach. The heading error estimation is shown in Fig. 14. The proposed fusion method has less heading error compared to the other methods. The mean heading error for magnetometer based approach is 18.55 degrees and for azimuth based approach is 7.48 degrees. The mean heading error for proposed method is 4.72 degrees. The experimental results show that the proposed heading fusion method reduced the sensor errors.

To evaluate the performance and accuracy of our proposed position-estimation algorithm, we considered three-experiment scenarios such as rectangular motion, straight-line motion, and circular motion of pedestrian. Fig. 15 depicts the trajectories of the ground truth, the conventional PDR approach, and proposed PDR approach for three-experiment scenarios. For the conventional PDR approach, acceleration based step detection approach (ZC) is used for the step detection. The step length is estimated by Weinberg [49] approach, (22) is used for heading estimation. Finally, (32) and (33) are used for position estimation. In order to validate our proposed position-estimation algorithm, we carried out our first experiment in the rectangular motion. In this experiment, the pedestrian walked in the rectangular direction. The experiment was carried out strictly along the reference path in our college building corridor. Fig. 15(a) shows the experimental results. The starting point is 10 m far from the corner of the building. The length of the path is 45 m and the width is 37 m. The red line shows the reference path. The proposed algorithm result shows high position accuracy than the position estimation from conventional method. The next experiment is the straight-line motion of the pedestrian. In this case, the pedestrian walked in the college building corridor in a straight direction. The experiment result shows that the proposed algorithm achieves better results compared to the conventional method. Fig. 15(b) shows the straight-line experiment result. The last experiment is the circular motion of the pedestrian. In this case, the pedestrian walked in a 9-m-radius circle. Fig. 15(c) shows the experiment result. The pedestrian walked in the reference circle path and the experimental result shows that the position from proposed algorithm has a high position accuracy compared to the conventional method. In this experiment, the starting point is origin and the red circle shows the reference circle path.

The accuracy of the proposed position-estimation algorithm is assessed and evaluated by displacement and root mean square error. The displacement errors are calculated by the difference between the starting and finishing points. Table 2 gives the displacement errors for rectangular and circular motion of the pedestrian.

TABLE 2. Displacement error.

Pedestrian Motion	Displacement error	
	Proposed Method	Conventional Method
Rectangular Motion	1 m	2.123 m
Circular Motion	0.67 m	4.9 m

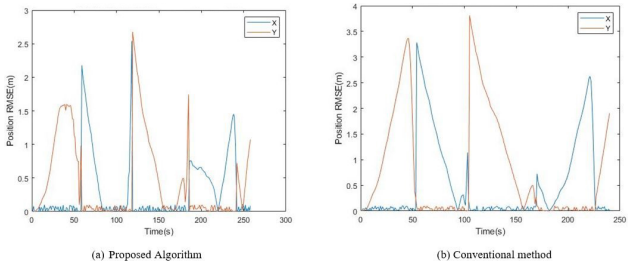

FIGURE 16. RMSE for position in rectangular motion.

From the table, the proposed algorithm has less displacement errors compared to the conventional method. The proposed algorithm reduced the displacement error. The RMSE calculates the position errors. Fig. 16 shows the RMSE for position in rectangular motion. The maximum error from the proposed position-estimation algorithm is 2.6 m. The maximum error from conventional method is 3.8 m. The proposed algorithm reduced the position error. The RSME of position in straight-line motion of pedestrian is shown in Fig. 17.

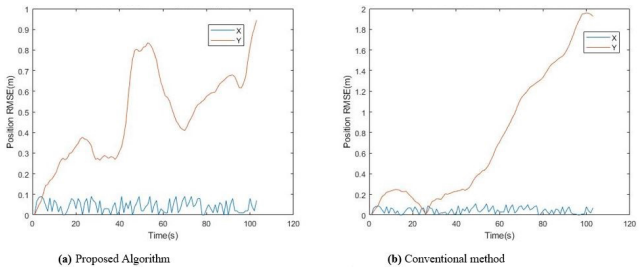

FIGURE 17. RMSE for position in straight-line Motion.

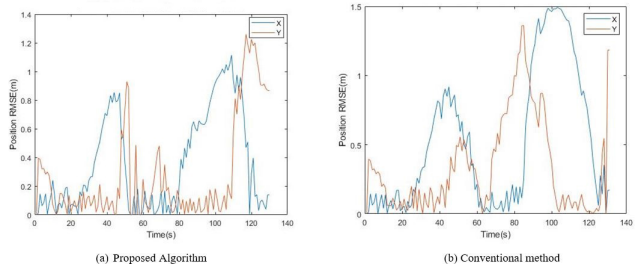

FIGURE 18. RMSE for position in circular motion.

TABLE 3. RMSE of position.

Pedestrian Motion	Maximum Position Error (m)			
	Proposed Method		Conventional Method	
	x	y	x	y
Rectangular Motion	2.5	2.6	3.2	3.8
Straight line Motion	0.94	0.09	1.95	0.11
Circular Motion	1.1	1.2	1.3	1.4

The maximum error in straight-line motion of pedestrian is 0.944 m by the proposed method and the maximum error from conventional method is 1.95 m. The proposed algorithm yields less position error compared to the conventional method. The RSME of position for the circular motion of a pedestrian is represented in Fig. 18. The maximum error is 1.2 m by the proposed method and the maximum error from the conventional method is 1.4 m. The proposed algorithm provides high position accuracy compared to the conventional method. Table 3 shows the x and y position errors for all experimental scenarios.

VI. CONCLUSION

This paper presented a position-estimation algorithm for indoor application. In comparison with other PDR algorithms, the proposed PDR algorithm shows high position accuracy for pedestrian motions. The proposed algorithm uses the complementary features of magnetometer and gyroscope and addressed the accumulated errors exist in PDR localization. In step detection procedure, we have proposed a pitch-based step detection by combining the accelerometer and gyroscope sensors. In heading estimation procedure, we have presented a sensor fusion technique by using gyroscope and magnetometer sensors. The proposed position-estimation algorithm was tested through three indoor experiments, and the results show that the proposed position-estimation algorithm shows high position accuracy. The rectangular motion experiment shows that the proposed position estimated path has a maximum of 2.6 m error when compared to the reference path. In the case of straight-line pedestrian motion, the experimental result shows that the proposed algorithm has a maximum of 0.94 m errors when compared to the ground-truth values. In the last experimental results, the proposed algorithm shows a maximum of 1.2 m errors when compared to the actual values. From the all experiments and results, the proposed algorithm shows high position accuracy as compared to the conventional method. However, in the future, we will carry out experiments in more complicated situations, such as pentagonal, hexagonal, or zigzag motion of pedestrians.

REFERENCES

[1] R. Xu, W. Chen, Y. Xu, and S. Ji, "A new indoor positioning system architecture using GPS signals," *Sensors*, vol. 15, no. 5, pp. 10074–10087, 2015.

[2] K. Özsoy, A. Bozkurt, and I. Tekin, "2D Indoor positioning system using GPS signals," in *Proc. Int. Conf. Indoor Positioning Indoor Navigat. (IPIN)*, Sep. 2010, pp. 1–6.

[3] J. Liu, R. Chen, L. Pei, R. Guinness, and H. Kuusniemi, "A hybrid smartphone indoor positioning solution for mobile LBS," *Sensors*, vol. 12, no. 12, pp. 17208–17233, 2012.

[4] L. Pei, J. Liu, R. Guinness, Y. Chen, H. Kuusniemi, and R. Chen, "Using LS-SVM based motion recognition for smartphone indoor wireless positioning," *Sensors*, vol. 12, no. 5, pp. 6155–6175, May 2012.

[5] M. Liu *et al.*, "Scene recognition for indoor localization using a multi-sensor fusion approach," *Sensors*, vol. 17, no. 12, p. 2847, 2017.

[6] Y. Zhuang, Z. Shen, Z. Syed, J. Georgy, H. Syed, and N. El-Sheimy, "Autonomous WLAN heading and position for smartphones," in *Proc. IEEE/ION Position, Location Navigat. Symp. (PLANS)*, May 2014, pp. 1113–1121.

[7] Y. Zhou, C. L. Law, Y. L. Guan, and F. Chin, "Indoor elliptical localization based on asynchronous UWB range measurement," *IEEE Trans. Instrum. Meas.*, vol. 60, no. 1, pp. 248–257, Jan. 2011.

[8] A. R. Jiménez and F. Seco, "Comparing decawave and bespoon UWB location systems: Indoor/outdoor performance analysis," in *Proc. Int. Conf. Indoor Positioning Indoor Navigat. (IPIN)*, Oct. 2016, pp. 1–18.

[9] Y. Zhuang, Z. Syed, J. Georgy, and N. El-Sheimy, "Autonomous smartphone-based WiFi positioning system by using access points localization and crowdsourcing," *Pervasive Mobile Comput.*, vol. 18, pp. 118–136, Apr. 2015.

[10] A. S. Paul and E. A. Wan, "Wi-Fi based indoor localization and tracking using sigma-point Kalman filtering methods," in *Proc. IEEE/ION Position, Location Navigat. Symp. (PLNS)*, May 2008, pp. 646–659.

[11] M. N. Husen and S. Lee, "Indoor location sensing with invariant Wi-Fi received signal strength fingerprinting," *Sensors*, vol. 16, no. 11, p. 1898, 2016.

[12] D. F. Llorca, M. A. Sotelo, I. Parra, M. Ocaña, and L. M. Bergasa, "Error analysis in a stereo vision-based pedestrian detection sensor for collision avoidance applications," *Sensors*, vol. 10, no. 4, pp. 3741–3758, 2010.

[13] N. Parnian and F. Golnaraghi, "Integration of a multi-camera vision system and strapdown inertial navigation system (SDINS) with a modified Kalman filter," *Sensors*, vol. 10, no. 6, pp. 5378–5394, 2010.

[14] S. Y. Kim, K. S. Yoon, D. H. Lee, and M. H. Lee, "The localization of a mobile robot using a pseudolite ultrasonic system and a dead reckoning integrated system," *Int. J. Control, Automat. Syst.*, vol. 9, no. 2, p. 339, Apr. 2011.

[15] M. Hazas and A. Hopper, "Broadband ultrasonic location systems for improved indoor positioning," *IEEE Trans. Mobile Comput.*, vol. 5, no. 5, pp. 536–547, May 2006.

[16] D. Sobers, S. Yamaura, and E. Johnson, "Laser-aided inertial navigation for self-contained autonomous indoor flight," in *Proc. AIAA Guid., Navigat., Control Conf. (GNC)*, Aug. 2010, p. 8211.
[17] S. S. Saab and Z. S. Nakad, "A standalone RFID indoor positioning system using passive tags," *IEEE Trans. Ind. Electron.*, vol. 58, no. 5, pp. 1961–1970, May 2011.
[18] S. House, S. Connell, I. Milligan, D. Austin, T. L. Hayes, and P. Chiang, "Indoor localization using pedestrian dead reckoning updated with RFID-based fiducials," in *Proc. Annu. Int. Conf. IEEE Eng. Med. Biol. Soc. (EMBC)*, Aug./Sep. 2011, pp. 7598–7601.
[19] A. R. J. Ruiz, F. S. Granja, J. C. P. Honorato, and J. I. G. Rosas, "Accurate pedestrian indoor navigation by tightly coupling foot-mounted IMU and RFID measurements," *IEEE Trans. Instrum. Meas.*, vol. 61, no. 1, pp. 178–189, Jan. 2012.
[20] J. Huang, X. Yu, Y. Wang, and X. Xiao, "An integrated wireless wearable sensor system for posture recognition and indoor localization," *Sensors*, vol. 16, no. 11, p. 1825, 2016.
[21] A. R. Jiménez, F. Seco, F. Zampella, J. C. Prieto, and J. Guevara, "PDR with a foot-mounted IMU and ramp detection," *Sensors*, vol. 11, no. 10, pp. 9393–9410, 2011.
[22] H. Yang *et al.*, "Smartphone-based indoor localization system using inertial sensor and acoustic transmitter/receiver," *IEEE Sensors J.*, vol. 16, no. 22, pp. 8051–8061, Nov. 2016.
[23] J. Benikovsky, P. Brida, and J. Machaj, "Localization in real GSM network with fingerprinting utilization," in *Proc. Int. Conf. Mobile Lightweight Wireless Syst.*, 2010, pp. 699–709.
[24] V. Otsason, A. Varshavsky, A. LaMarca, and E. de Lara, "Accurate GSM indoor localization," in *Proc. Int. Conf. Ubiquitous Comput.*, 2005, pp. 141–158.
[25] R. Górak, M. Luckner, M. Okulewicz, J. Porter-Sobieraj, and P. Wawrzyniak, "Indoor localisation based on GSM signals: Multistorey building study," *Mobile Inf. Syst.*, vol. 2016, Mar. 2016, Art. no. 2719576, doi: 10.1155/2016/2719576.
[26] A. Varshavsky, E. de Lara, J. Hightower, A. LaMarca, and V. Otsason, "GSM indoor localization," *Pervasive Mobile Comput.*, vol. 3, no. 6, pp. 698–720, 2007.
[27] R. Zhang, A. Bannoura, F. Höflinger, L. M. Reindl, and C. Schindelhauer, "Indoor localization using a smart phone," in *Proc. IEEE Sensors Appl. Symp. Proc. (SAS)*, Feb. 2013, pp. 38–42.
[28] Y. Liu, M. Dashti, M. A. A. Rahman, and J. Zhang, "Indoor localization using smartphone inertial sensors," in *Proc. 11th Workshop Positioning, Navigat. Commun. (WPNC)*, Mar. 2014, pp. 1–6.
[29] H.-H. Hsu, J.-K. Chang, W.-J. Peng, T. K. Shih, T.-W. Pai, and K. L. Man, "Indoor localization and navigation using smartphone sensory data," *Ann. Oper. Res.*, vol. 265, no. 2, pp. 187–204, 2018.
[30] E. Martin, O. Vinyals, G. Friedland, and R. Bajcsy, "Precise indoor localization using smart phones," in *Proc. 18th ACM Int. Conf. Multimedia (ICM)*, Oct. 2010, pp. 787–790.
[31] A. Abadleh, E. Al-Hawari, E. Alkafaween, and H. Al-Sawalqah, "Step detection algorithm for accurate distance estimation using dynamic step length," in *Proc. 18th IEEE Int. Conf. Mobile Data Manage. (MDM)*, May/Jun. 2017, pp. 324–327.
[32] N.-H. Ho, P. H. Truong, and G.-M. Jeong, "Step-detection and adaptive step-length estimation for pedestrian dead-reckoning at various walking speeds using a smartphone," *Sensors*, vol. 16, no. 9, p. 1423, 2016.
[33] Y. Liu, Y. Chen, L. Shi, Z. Tian, M. Zhou, and L. Li, "Accelerometer based joint step detection and adaptive step length estimation algorithm using handheld devices," *J. Commun.*, vol. 10, no. 7, pp. 520–525, 2015.
[34] X. Yuan, S. Yu, S. Zhang, G. Wang, and S. Liu, "Quaternion-based unscented Kalman filter for accurate indoor heading estimation using wearable multi-sensor system," *Sensors*, vol. 15, no. 5, pp. 10872–10890, May 2015.
[35] V. Renaudin, C. Combettes, and F. Peyret, "Quaternion based heading estimation with handheld MEMS in indoor environments," in *Proc. IEEE/ION Position, Location Navigat. Symp. (PLANS)*, May 2014, pp. 645–656.
[36] D. Liu *et al.*, "A novel heading estimation algorithm for pedestrian using a smartphone without attitude constraints," in *Proc. UPINLBS*, Nov. 2016, pp. 29–37.
[37] A. Ali and N. El-Sheimy, "Low-cost MEMS-based pedestrian navigation technique for GPS-denied areas," *J. Sensors*, vol. 2013, Jul. 2013, Art. no. 197090.
[38] W. Kang and Y. Han, "SmartPDR: Smartphone-based pedestrian dead reckoning for indoor localization," *IEEE Sensors J.*, vol. 15, no. 5, pp. 2906–2916, May 2015.
[39] Q. Tian, Z. Salcic, K. I-K. Wang, and Y. Pan, "A multi-mode dead reckoning system for pedestrian tracking using smartphones," *IEEE Sensors J.*, vol. 16, no. 7, pp. 2079–2093, Apr. 2016.
[40] B. Shin *et al.*, "Motion recognition-based 3D pedestrian navigation system using smartphone," *IEEE Sensors J.*, vol. 16, no. 18, pp. 6977–6989, Sep. 2016.
[41] H. Xia, Y. Qiao, J. Jian, and Y. Chang, "Using smart phone sensors to detect transportation modes," *Sensors*, vol. 14, no. 11, pp. 20843–20865, Nov. 2014.
[42] M. Zhang, Y. Wen, J. Chen, X. Yang, R. Gao, and H. Zhao, "Pedestrian dead-reckoning indoor localization based on OS-ELM," *IEEE Access*, vol. 6, pp. 6116–6129, 2018.
[43] P. Nguyen, T. Akiyama, H. Ohashi, G. Nakahara, K. Yamasaki, and S. Hikaru, "User-friendly heading estimation for arbitrary smartphone orientations," in *Proc. IPIN*, Oct. 2016, pp. 1–7.
[44] W. Koo, S. Sung, and Y. J. Lee, "Development of real-time heading estimation algorithm using magnetometer/IMU," in *Proc. ICCAS-SICE*, Aug. 2009, pp. 4212–4216.
[45] E. M. Diaz and A. L. M. Gonzalez, "Step detector and step length estimator for an inertial pocket navigation system," in *Proc. IPIN*, Oct. 2014, pp. 105–110.
[46] P. Kim, *Kalman Filter for Beginners: With MATLAB Examples*. Scotts Valley, CA, USA: CreateSpace, 2011.
[47] R. Zhou, "Pedestrian dead reckoning on smartphones with varying walking speed," in *Proc. ICC*, May 2016, pp. 1–6.
[48] L. Ilkovičová, P. Kajánek, and A. Kopáčik, "Pedestrian indoor positioning and tracking using smartphone sensors, step detection and map matching algorithm," in *Proc. Int. Symp. Eng. Geodesy*, Varazdin, Croatia, May 2016, pp. 1–24.
[49] E. Martin, "Novel method for stride length estimation with body area network accelerometers," in *Proc. IEEE Top. Conf. Biomed. Wireless Technol., Netw., Sens. Syst.*, Jan. 2011, pp. 79–82.
[50] K.-H. Yeh, "A secure IoT-based healthcare system with body sensor networks," *IEEE Access*, vol. 4, pp. 10288–10299, 2016.
[51] M. D. Shuster, "A survey of attitude representations," *Navigation*, vol. 8, no. 9, pp. 439–517, 1993.
[52] C.-H. Chen, C.-A. Lee, and C.-C. Lo, "Vehicle localization and velocity estimation based on mobile phone sensing," *IEEE Access*, vol. 4, pp. 803–817, 2016.
[53] S. Kianoush, S. Savazzi, F. Vicentini, V. Rampa, and M. Giussani, "Device-free RF human body fall detection and localization in industrial workplaces," *IEEE Internet Things J.*, vol. 4, no. 2, pp. 351–362, Apr. 2017.
[54] A. R. Pratama, W. Widyawan, and R. Hidayat, "Smartphone-based pedestrian dead reckoning as an indoor positioning system," in *Proc. ICSET*, Sep. 2012, pp. 1–6.
[55] Z. Chen, H. Zou, H. Jiang, Q. Zhu, Y. C. Soh, and L. Xie, "Fusion of WiFi, smartphone sensors and landmarks using the Kalman filter for indoor localization," *Sensors*, vol. 15, no. 1, pp. 715–732, 2015.

ALWIN POULOSE received the B.Sc. degree in computer maintenance and electronics from the Union Christian College, Aluva, India, in 2012, the M.Sc. degree in electronics from the MES College Marampally, India, in 2014, and the M.Tech. degree in communication systems from Christ University, Bengaluru, India, in 2017. He is currently pursuing the Ph.D. degree with the School of Electronics Engineering, Kyungpook National University, Daegu, South Korea. His research interests include indoor localization, activity recognition, and human behavior prediction.

ODONGO STEVEN EYOBU received the B.Sc. degree (Hons.) in computer science from Islamic University in Uganda, Mbale, Uganda, in 2005, the M.Sc. degree in data communications and software engineering from Makerere University, Kampala, Uganda, in 2009, and the Ph.D. degree from the School of Electronics Engineering, Kyungpook National University, Daegu, South Korea, in 2019. His research interests include vehicular communications, sensor and ad hoc networks, localization, and deep learning.

DONG SEOG HAN received the B.S. degree in electronic engineering from Kyungpook National University (KNU), Daegu, South Korea, in 1987, and the M.S. and Ph.D. degrees in electrical engineering from the Korea Advanced Institute of Science and Technology, Daejon, South Korea, in 1989 and 1993, respectively. From 1987 to 1996, he was with Samsung Electronics Co., Ltd., where he developed the transmission systems for QAM HDTV and Grand Alliance HDTV receivers. Since 1996, he has been with the School of Electronics Engineering, KNU, as a Professor. He was a courtesy Associate Professor with the Department of Electrical and Computer Engineering, University of Florida, in 2004. He was the Director with the Center of Digital TV and Broadcasting, Institute for Information Technology Advancement, from 2006 to 2008. His main research interests include intelligent signal processing and autonomous vehicles.